Hindawi
Mobile Information Systems
Volume 2019, Article ID 4383945, 15 pages
https://doi.org/10.1155/2019/4383945

Research Article

Assessing IEEE 802.11 and IEEE 802.16 as Backhauling Technologies for 3G Small Cells in Rural Areas of Developing Countries

Javier Simó-Reigadas,[1] **Carlos Figuera**,[1] **Eduardo Morgado**,[1] **Esteban Municio**,[2] **and Andrés Martínez-Fernández**[1]

[1]*Rey Juan Carlos University, Department of Signal Theory and Communications, Madrid, Spain*
[2]*IDLab—Department of Mathematics and Computer Science, University of Antwerp—IMEC, Antwerp, Belgium*

Correspondence should be addressed to Javier Simó-Reigadas; javier.simo@urjc.es

Received 27 June 2018; Accepted 9 December 2018; Published 17 January 2019

Academic Editor: Paolo Bellavista

Mobile networks are experiencing a great development in urban areas worldwide, and developing countries are not an exception. However, sparsely populated rural areas in developing regions usually do not have any access to terrestrial communications networks because operators cannot ensure enough revenues to justify the required investments. Therefore, alternative low-cost solutions are needed for both the access network and the backhaul network. In this sense, in order to provide rural 3G coverage in small villages, state-of-the-art approaches propose to use Small Cells in access networks and inexpensive multihop wireless networks based on WiFi for long distances (WiLD) or WiMAX for backhauling them. These technologies provide most of the required capabilities; however, there is no complete knowledge about the performance of WiFi and WiMAX in long-distance links under quality of service constraints. The aim of this work is to provide a detailed overview of the different alternatives for building rural wireless backhaul networks. We compare both IEEE 802.11n and IEEE 802.16 distance-aware analytical models and validate them by extensive simulations and field experiments. Also WiFi-based TDMA proprietary solutions are evaluated experimentally and compared. Finally, results are used to model a real study case in the Peruvian Amazon in order to illustrate that the performance provided by these technologies may be sufficient for the backhaul network of a rural 3G access network based on Small Cells.

1. Introduction

Although users would like to have universal and ubiquitous access to 3G services everywhere, operators limit the deployment of infrastructures to areas where revenues compensate the capital expenditures (CAPEX, mainly related to the deployment of infrastructures) and the operation expenditures (OPEX, including maintenance, operation, licenses, etc). Consequently, many large rural areas in developing regions that are sparsely populated lack 3G coverage, and often they do not even have any telecommunication services at all. Hence, in the context of the current trend towards ubiquitous communications worldwide, the need for more affordable 3G access and backhaul solutions becomes apparent.

Small Cells, which were initially conceived as a solution for coverage holes in urban areas, are now becoming a promising solution for rural access networks. Femtocells are generally used inside buildings and are designed to be low-cost, adaptable, and flexible and to have low power consumption so that a residential Asymmetric Digital Subscriber Line (ADSL) may be used as the backhaul. A 3G femtocell may be a suitable solution for the access network in a small village, since its cost and power consumption make it much more affordable for an operator than a common eNodeB. Therefore, a few small cells may ensure cellular coverage in most human settlements over a large sparsely populated region at a very low cost.

However, backhauling these 3G femtocells may become challenging. Many sparsely populated areas may be too far

from any well-connected location for a one-hop terrestrial link. This implicitly leaves only two alternatives: multihop broadband wireless networks or satellite communications. Although Very Small Aperture Terminal (VSAT) systems have a high OPEX and a round-trip delay over 500 ms (if geostationary communications satellites are used), they are commonly used as backhaul solutions for remote cellular spots; alternative terrestrial multihop wireless networks may be considered, but the cost is then a critical limitation. This trade-off attracts the interest on nonlicensed low-cost technologies compliant with wireless broadband standards IEEE 802.11 [1] (WiFi) and IEEE 802.16-2009 [2] (commonly known as WiMAX (although the WiMAX Forum does not have a profile for the WirelessHUMAN physical layer that describes the operation in nonlicensed bands)).

This is precisely the approach adopted by the project TUCAN3G [3] which proposes technically feasible but economically sustainable solutions for the progressive introduction of voice and broadband data services in small communities of rural areas of developing countries, using conventional 3G cellular terminals. Although 4G small cells (and 5G spots soon) may be a better solution in terms of the service level offered, they are also much more demanding in terms of backhaul capacity, which has a direct impact on cost effectiveness, so only 3G coverage will be considered in this paper.

Although the alternatives pointed out above are becoming more and more consistent and widely accepted [4], there is still a lack of accurate knowledge about the behaviour of alternative terrestrial backhaul technologies used under carrier-grade QoS (Quality of Service) requirements in long-distance links. For this reason, this paper analyses and compares the expected performance of WiFi, WiFi-based Time Division Multiple Access (TDMA) solutions, and WiMAX in long-distance links and determines for these technologies the conditions to be adequate as backhaul technologies for rural 3G femtocells. This is carried out by first studying their distance-aware analytical models and then comparing their performance through extensive simulations and few field tests in a real rural network. As a side contribution, we provide with the simulation platform used for testing these technologies as rural backhaul networks.

The reminder of this work is organized as follows. First, Section 2 introduces the problematic of a rural network and gives a general overview of the traffic requirements of a low-cost rural backhaul network. Section 3 presents the characteristics of three technologies that are relevant for their use as backhaul of 3G femtocells in rural areas: WiFi, WiFi-TDMA, and WiMAX. Section 4 presents the theoretical models adapted to long-distance links for WiFi and WiMAX systems, including specific simplifications for point-to-point (PtP) links. Section 5 summarizes the methods and conditions used to validate the theoretical models and to obtain the performance results that are presented in Section 6. Finally, Section 7 uses the performance results for validating the referenced technologies for their use in real scenarios such as rural backhaul network for 3G femtocells (the Napo network). Section 8 concludes this paper.

2. Motivation: Rural Wireless Backhaul Networks

A rural 3G access network based on femtocells requires of a backhaul solution with enough capacity and bounded delay, jitter, and packet-loss for an acceptable communication quality between the femtocells and the operator's network in which the HNB (Home Node B) controller resides.

The traffic supported by the backhaul in both directions contains three main aggregated traffic classes: high priority signalling traffic exchanged among the HNB and the controller, voice real-time traffic, and data. Of course, a more complex classification is possible because 'data' may include traffic of very different natures, but this three classes vision is general enough for the scope of this paper. The backhaul must have resources available in excess for high-quality transport for all the traffic or, alternatively, it must be able to prioritize signalling and voice traffic over more intensive data traffic, shaping the delay, jitter, and packet-loss as required for each traffic class.

In order to obtain a first overview of the capacity required for the backhaul of rural femtocells in developing regions, a prospective study was done in the frame of the TUCAN3G project [3] based on usage data obtained in covered areas in Peru. Although this study and its results are beyond the scope of this paper, there are some outcomes that are relevant to modelling the offered load for a backhaul transport network.

2.1. Voice Traffic. Approximately 50% of the people in rural areas are potential users of telephone, generating a traffic intensity of 15 mEr/user in the busy hour. With the blocking probability imposed to the operator in its regulation domain, this permits to calculate for a given access network the number of channels required in a coverage area for simultaneous phone calls. The throughput generated depends on the codec used and on the number of simultaneous calls. The AMR voice codec at 12.2 kbps is assumed, and circuit switch multiplexing is applied in the UL. Besides the payload, each packet also contains several headers for all the layers of the protocol stack: RTP, UDP, IPSec, and IP. Based on these considerations, the link-layer throughput is around 22 kbps in the UL and 60 kbps in the DL per phone call. For the case of the Peruvian regulatory context, a small village with only 500 inhabitants would need 9 voice channels, generating a throughput of 736 kbps of voice traffic in the busy hour. A large village with as much as 5000 inhabitants would require 48 voice channels, generating 3936 kbps in the busy hour. The calculations for other population figures are straight-forward.

2.2. Data Traffic. For data traffic, the potential market is approximately 5% of the population. A peak throughput per user of 3 Mbps must be ensured for a good quality of experience. The minimum capacity per user is 15 kbps (DL) + 5 kbps (UL). This means roughly that 3000 kbps must be available for all cases, and the capacity needs to grow proportionally to the population beyond 3000 inhabitants.

2.3. Signalling Traffic. Signalling between the HNB and the HNB controller has been carefully studied and is known to be lower than 1% of the traffic [3].

With the previous assumptions, it can be estimated that the required backhaul capacity of a 3G femtocell in a small village with less than 500 inhabitants must be at least 4.5 Mbps, and this requirement grows up slightly over 10 Mbps for a population of 5000 inhabitants. In fact, the data analysed come from areas where 3G coverage already exists, in which the average income of the population is higher than that in remote areas. Therefore, the projection overestimates the expected demand in very isolated areas.

ITU recommendations suggest certain end-to-end values for performance indicators in telephony [5]. 150 ms is a maximum limit for the one-way delay, and 2% is the maximum tolerable packet-loss. However, the backhaul has a share in these end-to-end values. As the access network and the core network may also introduce packet-loss and delay, in this paper, the backhaul contribution to these maximum values is considered limited to 0.8% for the packet-loss and 60 ms for the delay, which represent a contribution of 60% to the total values.

Finally, in this paper, we focused our study in the raw capacity and delay at the MAC layer. Therefore, we consider upper layers out of the scope of the work. On one hand, QoS provision has been already studied for rural backhaul networks in Simo-Reigadas et al. [6, 7], and hence, we assume that a number of mechanisms such as DiffServ, MPLS, or MPLS-TE exist for guaranteeing the requirements of each traffic type and their different applications. On the other hand, multihop routing is not addressed since it can be trivially implemented with standard well-studied proactive routing protocols such as OSPF or even with static routing. Finally, although we assume that the MAC links are encrypted with their correspondent L2 security protocol, we mainly relay in the security provided by the IPSec tunnels established in the Iuh 3GPP interface between the core network and the HNB. Accordingly, the authentication procedures are also transferred to the HNB and the access network.

3. Using WiLD and WiMAX as Backhaul Technologies in Rural Areas

3.1. WiLD (WiFi for Long Distances). The IEEE 802.11 standard [1], popularly known as WiFi (accurately speaking, WiFi is a commercial denomination for products certified by the WiFi Alliance as IEEE 802.11-compliant systems that meet certain requirements), is conceived for local and metropolitan area networks operating in 2.4 GHz or 5 GHz nonlicensed bands. The Medium Access Control (MAC) protocol used is Carrier Sense Multiple Access with Collision Avoidance (CSMA/CA), which is not well suited to long-distance communications. Nonetheless, some researchers have demonstrated that WiFi may also be used for long-distance links in rural areas, as far as line of sight (LOS) may be assured [8, 9]. Additionally, Reigadas et al. [9] proposed adjustments to CSMA/CA for optimal performance and showed in what conditions general analytical models are also valid for long distances. WiFi can be used normally with 20 MHz channels, but 5, 10, 40, and 80 MHz channels are also permitted. The standard includes several alternatives for the physical layer (PHY), being the High Throughput (HT) Orthogonal Frequency-Division Multiplexing (OFDM) PHY the one with best performance. Additionally, spatial diversity with Multiple Input Multiple Output (MIMO) can be used, and many commercial outdoor WiFi systems are prepared with dual antennas for MIMO 2×2. Depending on the received signal strength, different Modulation and Coding Schemes (MCSs) may also be used permitting different physical bitrates. For example, MIMO 2×2-enabled 802.11n systems can operate from a 6.5 Mbps bitrate (MCS0, 20 MHz channel, Single Input Single Output (SISO), 800 ns of guard interval in OFDM symbols) up to 300 Mbps (MCS15, 40 MHz channel, MIMO 2×2, 400 ns of guard interval). However, the actual saturation throughput at MAC layer is only a fraction of that PHY bitrate. Other interesting properties offered by WiFi are frame aggregation, which permits to integrate big bundles containing many frames in a single header, and traffic differentiation, which permits to prioritize some traffic classes over others.

No matter what MAC protocol is used, any communications solution with WiFi hardware can benefit from the spatial diversity in the HT PHY, which raises the question whether these benefits apply to long-distance LOS links or not. There is a flexible trade-off between diversity gain and multiplexing gain [10]. In order to benefit from any of them, the multiple spatial data streams transmitted in parallel must be highly independent. It is possible to achieve long-distance high-rank LOS MIMO channels, at the cost however, of an excessive size of towers to ensure the necessary separation between antennas [11, 12]. Nonetheless, cross polarization makes possible to obtain two orthogonal channels, especially in LOS scenarios and only slightly worsened with long distance [13–15].

3.2. 802.11n-Based Proprietary Solutions Using TDMA MAC. Some manufacturers of broadband wireless systems with IEEE 802.11 interfaces include as an option an alternative proprietary MAC protocol in their outdoor products for improved performance for long-distance links. Normally none of these proprietary MAC protocols is published with all the technical details. Only limited information is available in the datasheets provided and unbiased raw data from the vendors is usually difficult to obtain, since this may eventually lead to the data being used against the issuing company itself. However, implementations of academic proposals of this type like [16] permit to guess what these systems do. At a first glance, these products use common 802.11n cards with modified drivers that disable the CSMA/CA MAC, thus converting the wireless network interfaces in raw data transceivers that use the 802.11 PHY. On top of this, a simple TDMA Time-Division Duplexing (TDD) solution seems to be programmed. This TDMA protocol avoids contention, making the use of the wireless channel much more efficient at long distances.

Hence, these systems show a behaviour similar to WiMAX (see Section 3.3), having lower spectral efficiency, but with potentially higher capacity due to the wider channels they can use. Some researchers such as [16, 17] have proposed these WiFi-based solutions for outdoor long-distance links and [18] demonstrated that under similar conditions, this kind of solutions tends to be better than common WiFi for very long distances, while WiFi can be tweaked to be better for short and medium distances.

Among many others, Ubiquiti AirMAX [19] and Mikrotik NV2 [20] product families are extremely popular for long-distance links as low-cost powerful solutions. These systems can be experimentally tested, but, due to the proprietary nature of these solutions, it is not possible to either compare them theoretically or to extend the experimental results to other comparable solutions.

3.3. WiMAX for Long Distances. The IEEE 802.16 standard [2], popularly known as WiMAX (as for the case of WiFi, WiMAX is a certification given by the WiMAX Forum to products that are IEEE 802.16-compliant, that pass certain interoperability tests and that fit in certain profiles; the use of the WiMAX denomination in this paper is formally wrong because there is not any profile in the WiMAX Forum for products using the IEEE 802.16 WirelessHUMAN PHY; however, the term is used in the paper as a synonym of the standard to make it more readable), is conceived for metropolitan area networks, although the solution is also valid for rural broadband networks. The WirelessHUMAN PHY in the standard describes the operation in the 5 GHz non-licensed band. Other WiMAX profiles allow to operate in licensed bands, which is very relevant for these countries where the use of licensed bands in backhaul network is mandatory. However, although the 5G Hz band is more prone to interferences than licensed bands, its use for carried-grade service cannot be neglected due to the high-gain directive antennas used and the limited radio-frequency emissions present in unpopulated rural areas.

WiMAX uses OFDM at the PHY layer and TDM/TDMA with TDD for contention-free operation. Different traffic classes are recognized and can receive differentiated QoS guarantees. In WirelessHUMAN, channels can be as wide as 10 MHz. The capacity of a WirelessHUMAN link depends on the MCS (being BPSK 1/2 the slowest and 64 QAM 3/4 the fastest), the guard interval in OFDM symbols (1/4–1/32), the frame size (2.5–20 ms), and so on. A stable WiMAX link may have a raw capacity between 1.6 Mbps and 36 Mbps. The link distance impacts on the link budget, determining what MCS can be used, but has little impact on the performance otherwise. Regarding the use of spatial diversity, the same considerations previously explained for WiFi can also be extended to WiMAX.

Although WiLD, WiFi-TDMA, and WiMAX seem promising solutions for rural backhauls, there are not previous systematic analysis aiming to know the real MAC capacity in long-distance links and no works exist that compare their performance depending on the distance and on the real impact of the different features mentioned above. To the best of our knowledge, this work is the first in doing this.

4. Performance Analysis of IEEE 802.11 and 802.16 WirelessHUMAN Long Links

4.1. Modelling the Performance of 802.11 for Long Distances. Simo et al. [9] proposed an analytical model for long-distance WiFi links based on [21]. While the hints given in [9] for the adaptation of WiFi to long distances are valid for any standard of the 802.11 family, the performance model itself is not valid for 802.11n because of certain limitations inherited from Bianchi's model [21]. Bianchi revised his model and proposed a new one in 2010 [22] that can be applied to the different PHY in IEEE 802.11-2012, which can be summarized in the following equations:

$$\tau = \frac{1}{1 + \left(1 - p/2\left(1 - p^{R+1}\right)\right)\sum_{i=0}^{R} p^i \left(2^i W - 1\right) - \left(1 - p/2\right)}, \tag{1}$$

$$p = 1 - (1 - \tau)^{n-1}, \tag{2}$$

where p and τ are, respectively, the conditional collision probability and the probability of a station to transmit in any slot; W is a constant, corresponding with the highest possible value of the contention window for a packet that is being transmitted for the first time; and R is the number or retransmissions (not considering the first transmission) before dropping a frame and trying with the next; and n is the number of WiFi stations.

The previous analysis assumes an ideal channel in which packet-loss only occurs by collision when two or more stations transmit simultaneously. However, in real conditions, the wireless channel may cause significant packet-loss due to channel errors and interferences. Therefore, it is also necessary to take in account the Packet Error Rate (PER) in the model as previously done in other works [23, 24]. When using 802.11 as a backhaul technology in rural areas, interferences are not common, and packet-losses are also infrequent because modulation and coding schemes are chosen for having a large margin between RSSI (Received Signal Strength Indication) and Sensitivity. However, we can carry out a simple and practical analysis considering that a transmitting WiFi station is unable to distinguish whether a transmitted packet has not reached its destination due to collision or the packet has arrived but with errors. In both cases, the transmitting station takes the same actions to retransmit the packet [25, 26]. Thus, we can just redefine p as the probability that a packet should be retransmitted either by collision or errors in the channel, and (2) becomes

$$p = \left(1 - (1 - \tau)^{n-1}\right)(1 - \text{PER}) + \text{PER}. \tag{3}$$

This set of equations cat be solved numerically. For the case of ideal channels, Table 1 shows the results for the most important values of W that can be considered here (the default values for the different PHYs), for the standard number of retransmissions (7 for basic mode, 4 for RTS/CTS mode), and for up to 5 stations. For the case of real channels,

Table 1: Values of p and τ calculated from (1) and (2).

n	$W=4$		$W=8$		$W=16$		$W=32$	
	p	τ	p	τ	p	τ	p	τ
2	0.289	0.289	0.188	0.188	0.109	0.109	0.058	0.058
3	0.383	0.214	0.280	0.151	0.183	0.096	0.106	0.054
4	0.438	0.174	0.337	0.128	0.236	0.085	0.146	0.051
5	0.477	0.149	0.377	0.111	0.276	0.077	0.180	0.048

Tables 2 and 3 show the corresponding results considering PER = 0.01 and 0.1, respectively. It is important to notice that PER = 0.1 is actually a maximum value because the standard uses it for the definition of sensitivity and determines that a link should not be established with higher PER values.

This model is valid for long-distance links, conditioned to the adjustment of SlotTime, ACKTimeout, and CTSTimeout MAC parameters as indicated in [9].

Based on the values of p and τ obtained from (1) and (3), the equations proposed in Section 5 of [22] for the saturation throughput and for the delay are valid with some remarks:

(i) The SlotTime δ must be replaced in all expressions by δ_d following indications in [9].

(ii) The time durations used in the throughput equation must be redefined considering the propagation time T_p, calculated consistently with [9].

Then,

$$E[T_s] = \delta_d + \frac{W}{W-1}\left(T_{MPDU} + SIFS + T_{ACK} + DIFS + 2T_p\right),$$
$$E[T_c] = \delta_d + \left(T_{MPDU} + SIFS + T_{ACK} + DIFS + T_p\right), \quad (4)$$

for basic mode, or

$$E[T_s] = \delta_d + \frac{W}{W-1}\left(T_{RTS} + T_{CTS} + T_{MPDU} + 3T_{SIFS} + T_{ACK} + T_{DIFS} + 4T_p\right), \quad (5)$$
$$E[T_c] = \delta_d + \left(T_{RTS} + T_{CTS} + SIFS + DIFS + T_p\right),$$

for RTS/CTS mode.

The model in [9] modified by the previous equations permits to obtain the saturation throughput and delay for WiFi links at any distance. This result provides the maximum capacity at link level. The following subsections will use the saturation point as a reference to find an optimal unsaturated operation point that keeps the delay under a threshold that is adequate for a backhaul link. The model will be used as a reference to validate the NS3 simulator, which is the tool that allows to accurately study the performance of long-distance links in a flexible manner.

4.1.1. Simplified WiLD Model for a PtP Setup. The previous model is valid for n stations, and doing $n = 2$, we obtain a PtP model where (3) becomes

Table 2: Values of p and τ calculated from (1) and (3) with PER = 0.01.

n	$W=4$		$W=8$		$W=16$		$W=32$	
	p	τ	p	τ	p	τ	p	τ
2	0.293	0.286	0.194	0.186	0.116	0.107	0.067	0.057
3	0.386	0.212	0.284	0.150	0.189	0.095	0.114	0.054
4	0.440	0.173	0.340	0.126	0.241	0.084	0.153	0.051
5	0.479	0.148	0.380	0.110	0.280	0.076	0.186	0.048

Table 3: Values of p and τ calculated from (1) and (3) with PER = 0.1.

n	$W=4$		$W=8$		$W=16$		$W=32$	
	p	τ	p	τ	p	τ	p	τ
2	0.330	0.256	0.248	0.165	0.186	0.095	0.146	0.051
3	0.413	0.192	0.324	0.133	0.245	0.084	0.184	0.048
4	0.463	0.158	0.373	0.113	0.288	0.075	0.216	0.045
5	0.500	0.136	0.408	0.099	0.321	0.068	0.243	0.042

$$p = \tau + PER(1-\tau). \quad (6)$$

This leads to validate performance results for a PtP WiLD link under saturation conditions. Although the model used is based on the hypothesis of n being higher, simulations have proved that the incremental error using the model for $n = 2$ (point-to-point case) is negligible.

4.2. Modelling the Performance of WiMAX. In this section, we develop a theoretical model for computing the performance of IEEE 802.16 WirelessHUMAN. First, we present a general model which accounts for different number of stations, several strategies for packing the information in the MAC level, and the possibility of including a MIMO radio interface. All the computations are based on information gathered from the IEE802.16-2009 standard [2] and the analysis in [27]. Table 4 collects the main parameters used in this analysis.

802.16 WirelessHUMAN profile [2] assumes OFDM modulation with $N = 256$ subcarriers. Only $N_{data} = 192$ of them are used for data. A cyclic prefix of length $CP \cdot N$ is used to avoid intersymbol and intercarrier interference. Given the sampling frequency $F_s = n_s B$ which depends on the channel bandwidth B and the sampling factor n_s, the duration of one OFDM symbol is $T_{OFDM} = N(1 + CP)/(n_s B)$. Each OFDM symbol transmits with only one MCS with modulation order M and coding rate r. Defining the function $\beta(r, M) = N_{data} r \log_2(M)$ as the bits carried by an OFDM symbol, the raw bitrate supported by the OFDM modulation is

$$R_{PHY}^{(raw)} = \frac{\beta(r, M)}{T_{OFDM}}. \quad (7)$$

Available MCSs are shown in Table 5. If MIMO is used, a maximum multiplexing gain $G_{max} = \min(M_t, M_r)$ can be obtained, where M_t and M_r are the number of transmitter and receiver antennas, respectively. Assuming that more than one antenna is present both in the transmitter and

Table 4: WiMAX model and simulation parameters.

Parameter	Description	Value (std.)	Value (exper.)
T_p	Air propagation time	$(D[m]/300)$	—
N	Subcarriers	256	—
N_{data}	Subcarriers used for data	192	—
B	Channel bandwidth	—	10 MHz
n_s	Sampling factor	—	144/125
CP	Cyclic prefix length	1/32 to 1/4	1/4
T_f	Frame duration	2.5 to 20 ms	2.5 ms
TTG	Transmit/receive transition gap	—	100 μs
RTG	Receive/transmit transition gap	—	100 μs
f^{DL}	Fraction of time for downlink	—	0.5
(M, r)	(Modulation order, coding rate)	(2, (1/2))–(64, (3/4))	—
S_{RNG-OP}	Ranging op. Duration (OFDM symbols)	To	$\max(1, 2 \times T_p)$
MTU	Maximum transmission unit	≤1400 bytes	1400 bytes

Table 5: Sensitivities from typical equipment used to compare the different technologies for SISO and MIMO [28, 29].

Sensitivity (dBm)			
Wifi and NV2		WiMAX	
MCS0	−96	BPSK 1/2	−92
MCS1	−95	QPSK 1/2	−91
MCS2	−92	QPSK 3/4	−89
MCS3	−90	16 QAM 1/2	−87
MCS4	−86	16 QAM 3/4	−84
MCS5	−83	64 QAM 2/3	−80
MCS6	−77	64 QAM 3/4	−76
MCS7	−74	—	—
MCS8	−95	BPSK 1/2	−94
MCS9	−93	QPSK 1/2	−93
MCS10	−90	QPSK 3/4	−92
MCS11	−87	16 QAM 1/2	−89
MCS12	−84	16 QAM 3/4	−85
MCS13	−79	64 QAM 2/3	−81
MCS14	−78	64 QAM 3/4	−79
MCS15	−75	—	—

receiver, the actual multiplexing gain G will depend on the MIMO configuration [2] and the statistical dependence among channels, so $1 \le G \le G_{max}$. Then, raw physical rate would be given by $R^{(raw)}_{PHY,MIMO} = R^{(raw)}_{PHY} G$.

Raw physical rate is diminished due to frame structure. First, time gaps RTG (Receive/transmit Transition Gap) and TTG (Transmit/receive Transition Gap) allow the transceiver to switch between transmission and reception. If TDD is used, temporal split between downlink (DL) and uplink (UL) can be modified. We denote f^{DL} for the fraction of useful transmission time which is used for DL and T_f for the frame duration. Then, the number of OFDM symbols in the DL and UL can be computed as

$$S^{DL}_{raw} = \left\lfloor \frac{(T_f - TTG - RTG) f^{DL}}{T_{OFDM}} \right\rfloor,$$
$$S^{UL}_{raw} = \left\lfloor \frac{(T_f - TTG - RTG)(1 - f^{DL})}{T_{OFDM}} \right\rfloor. \quad (8)$$

In the DL, the frame begins with a preamble (2 symbols) and the Frame Control Header (FCH) field (1 symbol). Then, a broadcast (BC) burst is transmitted which contains the UL-MAP, the DL-MAP, and the downlink and uplink channel descriptors (DCD and UCD, respectively). The length of these fields depends on the number of modulations and users that are active in a frame, and the number of optional variable-length messages which are used. Therefore, the most relevant overhead in the BC burst is due to

(i) UL-MAP: $b_{UM} = 64 + 48(N_{ss} + 2)$ bits (mandatory every frame), where N_{ss} is the number of active subscribers in that frame;

(ii) DL-MAP: $b_{DM} = 64 + 32N_{ss}$ bits (optionally every frame);

(iii) UCD and DCD: $b_{DCD} = 16 + 24N^{DL}_b$ bits $b_{UCD} = 16 + 24N^{UL}_b$ where N^{DL}_b and N^{UL}_b are the numbers of bursts which are scheduled in the DL and the UL, respectively, and are usually different.

Note that the transmission frequency for the channel descriptors f_{CD} depends on the channel coherence time and the implementation. The number of OFDM symbols used for the BC burst is

$$S_{BC} = \left\lceil \frac{b_{UM} + b_{DM} + (b_{DCD} + b_{UCD}) f_{CD}}{\beta(r_{BC}, M_{BC})} \right\rceil, \quad (9)$$

where $M_{BC} = 2$ and $r_{BC} = 1/2$ are the modulation order and coding rate for the BC burst, respectively. The BC burst and the users' bursts are optionally preceded by a short 1-symbol preamble. If we consider that each user is assigned a single burst, the number of symbols in the DL that can be used for MAC data is

$$S^{DL} = S^{DL}_{raw} - (2 + 1 + S_{BC} + 1(N_{ss} + 1)). \quad (10)$$

In the DL, the following fields reduce the number of available OFDM symbols:

(i) *Ranging* ($S_{RNG} = S_{RNG-OP} N_{RNG-OPS}$). A variable number of opportunities $N_{RNG-OPS}$ are given for user ranging. The duration of each one S_{RNG-OP} depends on the maximum user distance allowed in the cell and the particular implementation.

(ii) *Bandwidth request (S_{BR}).* A variable number of 2-symbol length bandwidth request is scheduled in the UL to allow users to request bandwidth for each connection.

(iii) A 1-symbol preamble is placed before each UL burst.

If we consider that each user is assigned to a different burst, the number of symbols in the UL that can be used for MAC data is

$$S^{\mathrm{UL}} = S^{\mathrm{UL}}_{\mathrm{raw}} - \left(S_{\mathrm{RNG}} + S_{\mathrm{BR}} + N_{\mathrm{ss}}\right). \tag{11}$$

In a particular frame $\mathscr{B}^{(x)}$, bursts are transmitted in the x direction, with $x \in \{\mathrm{DL}, \mathrm{UL}\}$ a variable introduced to simplify the notation. Each burst carries $S_b^{(x)}$ OFDM symbols, each one with a MCS defined by the coding rate $r_b^{(x)}$ and the modulation order $M_b^{(x)}$, with b the burst index. The number of bursts and the MCS for each one depends on the QoS needs and the channel state for each user, and the following equalities must hold: $\sum_{b=1}^{\mathscr{B}^{(x)}} S_b^{(x)} = S^{(x)}$. Then, the net rates provided by the PHY to the MAC level are computed as

$$R^{(x)}_{(\mathrm{PHY})} = \frac{b^{(x)}}{T_{\mathrm{f}}}, \tag{12}$$

with $b^{(x)}$ the number of bits that are available for MAC PDUs in the x direction, which is given by

$$b^{(x)} = \sum_{b=1}^{\mathscr{B}^{(x)}} S_b^{(x)} \beta\left(r_b^{(x)}, M_b^{(x)}\right). \tag{13}$$

Once the PHY operation has been modelled, the rest of this subsection is going to focus on the MAC layer. The subsequent analysis is valid for the DL and UL. The main overheads introduced in the MAC level are (i) the MAC PDU header (6 bytes) and CRC (4 bytes), so the overhead is $O_{\mathrm{PDU}} = (6 + 4)8$ bits and (ii) the Packing Subheader ($O_{\mathrm{PSH}} = 2$ bits) before each SDU, if packing is enabled. Also, several management messages are sent as MAC PDUs, including functionalities like ARQ and H-ARQ. Finally, other secondary subheaders are described in the standard for different signalling procedures. Since management messages and secondary subheaders are not very frequent, we only consider the PDU header and CRC and the Packing subheaders.

In the MAC level, each burst may carry one or more PDUs, depending on whether the MAC SDUs packing functionality is enabled. If packing is enabled, several MAC SDUs are packed in a unique PDU, and usually only one MAC PDU exists per burst. If not, one MAC SDU is encapsulated using one MAC PDU, and several PDUs exist in a burst. Let us denote $\mathscr{P}_b$ as the number of PDUs in the b-th burst and $\mathscr{D}_{b,p}$ as the number of SDUs in the p-th PDU of the b-th burst. Under these assumptions, the MAC overhead in the b-th burst in the x direction is computed as

$$O_b^{(x)} = O_{b,\mathrm{PAD}} + \sum_{p=1}^{\mathscr{P}_b} O_{\mathrm{PDU}} + \mathscr{D}_{b,p} O_{\mathrm{PSH}}, \tag{14}$$

where $O_{b,\mathrm{PAD}}$ are padding bits in order to complete the last OFDM symbol of the b-th burst.

Finally, the MAC rate for the x direction is computed as

$$R^{(x)}_{\mathrm{MAC}} = \left(\sum_{b=1}^{\mathscr{B}^{(x)}} S_b^{(x)} \beta\left(r_b^{(x)}, M_b^{(x)}\right) - O_b^{(x)}\right) \frac{1}{T_{\mathrm{f}}}. \tag{15}$$

4.2.1. Simplified WiMAX Model for a PtP Setup. If WiMAX is used in a PtP link, only one subscriber is connected to the base station ($N_{\mathrm{ss}} = 1$), and several simplifications in the model may be done. Moreover, in order to compare the model with our simulations and experiments, we use the specific configuration used during the tests. First of all, for only one user, the DL-MAP is optimized by carrying scheduling information in the Downlink Frame Prefix (DLFP) and reducing the length of the DL-MAP to only 32 bits. Regarding the DCD and the UCD, a fixed number of $N_b^{\mathrm{DL}} = 7$ and $N_b^{\mathrm{UL}} = 11$ bursts, respectively, are considered by the hardware. However, only one frame, each 1200 ms, carries these two fields. In the UL, one ranging opportunity and two bandwidth request opportunities are provided by default, although these are configurable by software. Since only one user is active, the number of bursts is one, and the number of bits available for MAC PDU's in (13) is simplified as $b^{(x)}_{\mathrm{PHY}} = S^{(x)} \beta(r^{(x)}, M^{(x)})$, where the number of symbols $S^{(x)}$ are computed by taking into account the assumptions made above, and $r^{(x)}$ and $M^{(x)}$ are the coding rate and modulation used for each direction.

In the MAC level, SDU packing is enabled in our device, and only one PDU is carried in the only burst in the subframe. Hence, MAC overhead is now computed as $O^{(x)} = O_{\mathrm{PAD}} + O_{\mathrm{PDU}} + \mathscr{D}^{(x)} O_{\mathrm{PSH}}$, where O_{PAD} accounts for the padding bits, and $\mathscr{D}^{(x)}$ is the number of MAC SDU's that are packed in a subframe. The latter can be computed as

$$\mathscr{D}^{(x)} = \left\lceil \frac{b^{(x)}_{\mathrm{PHY}} - O_{\mathrm{PDU}}}{\mathrm{MTU} + O_{\mathrm{PSH}}} \right\rceil, \tag{16}$$

where the ceil operator is used since we assume that fragmentation is enabled and MTU is the maximum transmission unit, which equals the SDU length in our setup. Finally, the MAC rate is computed as

$$R^{(x)}_{\mathrm{MAC}} = \left(b^{(x)}_{\mathrm{PHY}} - O^{(x)}\right) \frac{1}{T_{\mathrm{f}}}. \tag{17}$$

5. Measuring the Performance of the Technologies Being Assessed

Once the WiLD and WiMAX performance models have been described, we validate them comparing theoretical results with an external reference. On one hand, the use of the distance as a fundamental variable, with objective values in the range 0–60 km, makes almost impossible to run extensive tests with real equipments at arbitrary distances. On the other hand, it is necessary to extend the capability of measuring performance indicators to any distance, with any configuration and under any traffic load.

For these reasons, a simulator can be used to cross validate both the models, obtaining results for a more

realistic and wider set of scenarios and configurations. The event-driven NS-3 network simulator [30] has been chosen as the most widely used in research on wireless networks (the code and scripts implemented for this work for testing long-distance point-to-point links for WiLD and WiMAX in NS-3 are available in https://github.com/emunicio/long-distance-tucan3g). Finally, laboratory and field tests, although limited to 0 km (5 m) and 30 km (29.8 km), will additionally permit to cross check these simulation results as well. Note that in this work, where we use the term 0 km, we always mean 5 meters, and for the experiments at 30 km, we mean actually 29.8 km.

For NV2 and AirMAX systems, the lack of information about the implemented protocols and algorithms in these proprietary solutions makes impossible both theoretical analysis and software simulation. A testbed in laboratory has permitted to measure the performance at short distances, and the small knowledge about this technology together with punctual measurements on a few long-distance real links has been the base for projections that permit to estimate the expected performance at any distance in the range of interest. Mikrotik RouterBoard R52Hn with MIMO 2 × 2 capabilities has been used for experimenting with the 802.11n PHY layer, both with the standard CSMA/CA MAC layer and with the proprietary NV2 MAC layer, and Ubiquiti Rocket M5 systems have been used for testing AirMAX.

We have performed all tests in the 5 GHz band, injecting traffic with D-ITG [31]. Since NV2 and AirMAX have shown equivalent performance in the experiments, only NV2 has been retained for comparison with WiLD and WiMAX. A few WiMAX experiments have also been run in order to validate theoretical calculations and simulations at short distances, using Albentia ARBA PRO 4900–5875 MHz base station and subscriber stations.

For simulations of WiLD links with NS-3, AckTimeout and CTSTimeout values have been correctly set as explained in [9]. Table 5 shows the typical specifications in WiLD, WiMAX, and NV2 equipment. Table 6 shows the parameters taken to estimate the link budget. We have used a bidirectional UDP static flow for both the simulations and the experimental tests. We focus our performance analysis in raw capacity as backhaul links. For performance analysis for different applications and traffic types and under QoS constraints in rural backhaul networks, we refer to our previous works [6, 7]. Finally, other performance metrics can be easily obtained with the same tools as done in previous works [32, 33].

Table 6: Parameters used to estimate link budgets.

Link budget parameters	
Transmission power	24 dBm
Directional antenna gain	27 dB
Cable and connectors attenuation	2 dB
Margin	20 dB

6. Performance Results

6.1. Cross-Validating the Analytical WiLD Model and NS-3. In this subsection, we present comparative results between the model, the NS-3 simulator, and the performed experimental tests. The tests have been done by saturating a point-to-point link bidirectionally with UDP packets with 1372 bytes of payload, without neither frame aggregation nor Block-ACK, using 20 MHz of bandwidth and adapting the SlotTime to the distance as indicated in [9]. The Guard Interval is set to 800 ns in all cases. Each sample corresponds to the averaged value of 20 samples (simulation and experiments).

Figure 1(a) shows the saturation throughput achieved by WiLD as the distance is increased. For the sake of clarity, we only represent the results with the lowest and highest MCS with SISO and MIMO 2 × 2, i.e., MCS0 and MCS7, and MCS8 and MCS15, respectively. Continuous and dashed lines represent the results obtained through the analytical model and the NS-3 simulator, respectively. It can be seen that the differences between analytical model and simulation are negligible, specially for the lower MCSs. Figure 1(a) shows also the saturation throughput achieved in experimental tests in laboratory conditions at a distance of 0 km. Although the IEEE 802.11 implementation in NS-3 has been already widely validated by a number of works [34, 35], we show that our preliminary results also confirm the match between the three approaches.

6.2. Cross-Validating the Analytical Model for WiMAX and NS-3. Tests and calculations have been done saturating a point-to-point link bidirectionally with UDP packets with 1372 bytes of payload, using the most efficient frame duration and cyclic prefix: frame length of 20 ms and cyclic prefix of 1/32. The UL/DL ratio is set to 50%. Results are obtained experimentally for a distance of 0 km (5 m) in laboratory, and for all distances for the analytical model and for NS-3. Figure 1(b) represents the aggregated saturation throughput of UL and DL for MCS from BPSK 1/2 up to 64 QAM 3/4. At a distance of 0 km, the experimental measurements and the simulations match fairly well, and the results obtained with the analytical model are also very close to the experimental results (errors under 1% for the worst case, with frame duration of 20 ms). It is convenient to indicate that WiMAX systems have many more implementation specific options that condition the performance importantly, and only manufacturers know the exact adjustments for their products.

6.3. Results Obtained for WiLD. The aim of this subsection is to determine what is the optimal performance of IEEE 802.11n depending on the distance for long point-to-point links and how it can be achieved. There are two main questions that have to be answered: what is the dependence of the capacity on the frame aggregation and what is the expected delay depending on the load level.

Figure 2(a) presents the saturation throughput achieved for different frame aggregation levels. The Guard Interval is 800 ns, the bandwidth is 20 MHz, and UDP packets with a payload of 1372 bytes are injected bidirectionally in order to saturate the link. N is the number of packets aggregated per

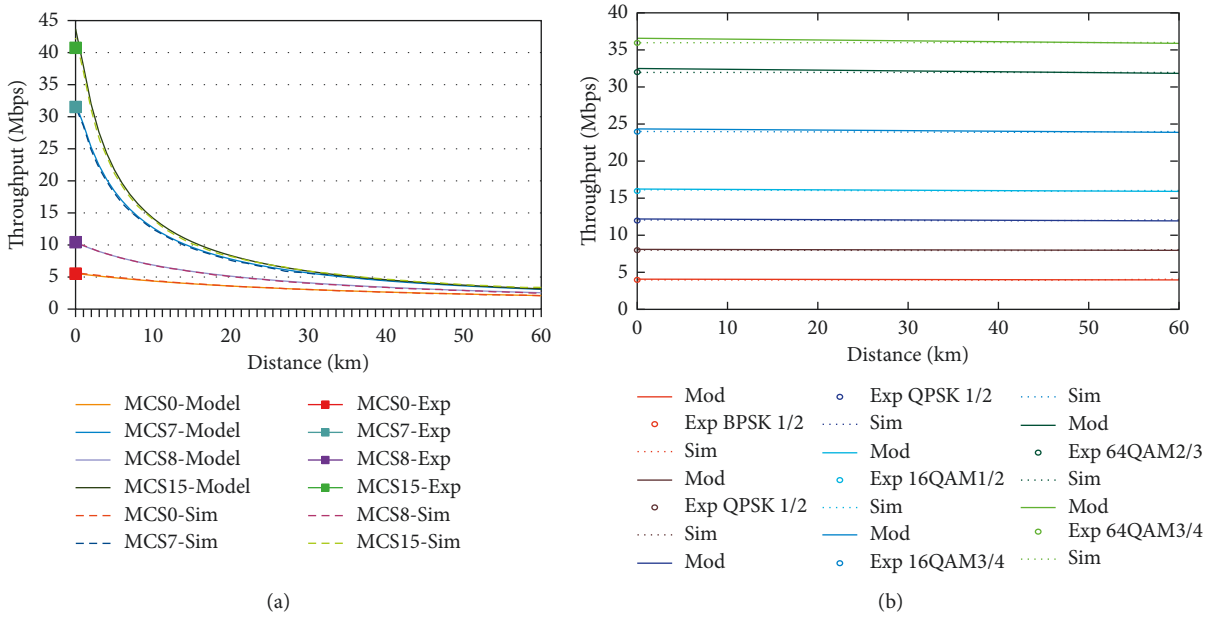

FIGURE 1: Average saturation throughput values obtained with the model, NS-3 simulator and experimental tests regarding the distance. (a) WiLD Throughput without frame aggregation. (b) WiMAX Throughput with 20 ms of frame duration and 1/32 CP.

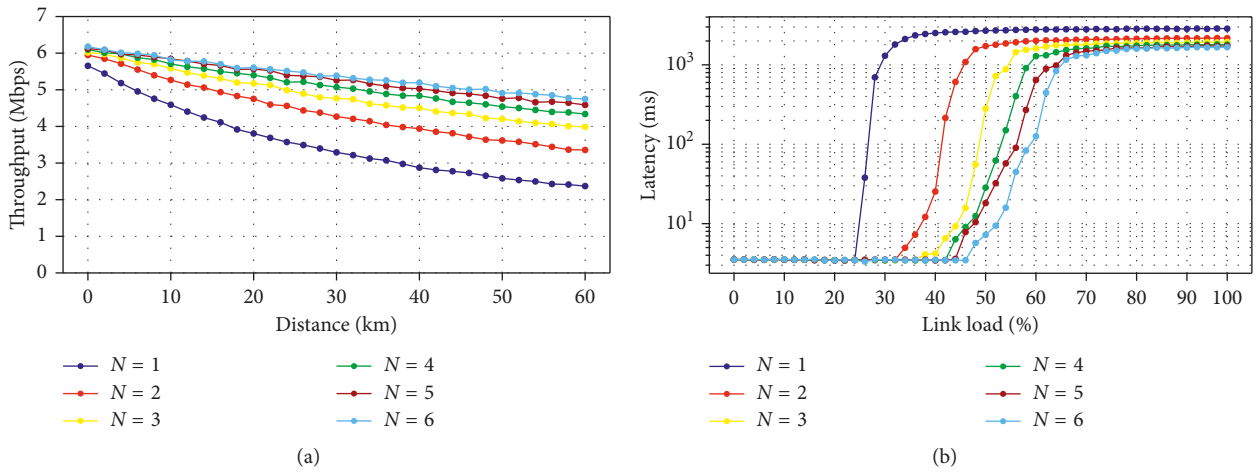

FIGURE 2: Simulation results for WiFi. (a) Average saturation throughput values for different frame aggregation thresholds. (b) Average delay values for different frame aggregation thresholds regarding the load at a distance of 30 km.

transmission. Although the standard permits to achieve higher levels of aggregation, many implementations have a maximum threshold of 8192 bytes/block, and the results show that the advantage of $N > 5$ is little in terms of capacity. From Figure 2(a), the interest of using frame aggregation with the highest possible value becomes apparent.

In order to represent how the average delay changes with the frame aggregation level, the distance has been fixed to 30 km, and the results are given in Figure 2(b). The X axis represents the offered load as a percentage of the nominal bitrate, where 100% represents the PHY throughput of a given MCS at a given distance. MCS0 is used in this case, and the rest of parameters are the used ones for the previous Figure 2(a)).

It can be seen that the advantage of the frame aggregation in terms of capacity is at no cost in terms of latency. The curves of latency (log scale) are very characteristic and drive to some clear conclusions. The delay is low (around 3 ms in the simulations and experiments) up to a point where it grows up to values of more than 1 second. This high increase in latency is basically due to the queuing delay originated when CDMA/CA is at its limit and collisions (although $n = 2$, traffic is bidirectional) reduce the channel efficiency. This reveals that although the throughput can be increased substantially up to a maximum saturation throughput value (100% of the link capacity), it is advisable to keep the load of the link below the saturation point (i.e., below the 50% of the actual maximum throughput, in

the flat part of Figure 2(b)), so that the delay stays bounded under low delay figures.

Additionally, the packet-loss is zero up to that saturation point and increases linearly beyond that point. This is specially crucial if the link is used for backhauling traffic from 3G cells, where the QoS requirements of telephone enforce the use of the link only in the low-latency region (as seen in the previous subsection). For example, the theoretical bitrate for MCS0 is 5.5 Mbps at MAC level, but the maximum offered load for a 30 km link that keeps the average delay under 5 ms is 3.3 Mbps, which is approximately 55% of the nominal bitrate. By limiting the traffic in the link and keeping it under its saturation point, the capacity decreases, but permits to obtain a low delay and negligible packet-loss in exchange. That threshold must be known for all MCS and all distances. These values (shown in the following subsection) can be obtained with NS-3 and permit to associate any link (given distance and MCS) in the network to a maximum allowed traffic load [6, 7].

6.4. Results Obtained for WiMAX. The performance of WiMAX long-distance links depends on many parameters, and the adjustments for long point-to-point links are straight-forward for many of them. For example, there are different options for the bandwidth, being 10 MHz the highest in the 5 GHz nonlicensed band. As this is the widest bandwidth available, it will be the bandwidth used in all cases. Other parameters such as the cyclic prefix may depend on the specific context: the lowest cyclic prefix (1/32) permits to obtain the highest capacity, but it can only be used if reflections are not significant. The frame duration has to be studied more carefully. On one hand, a higher frame duration reduces the overhead, increasing the efficiency. On the other hand, the longer the frames, the higher the average delays.

Figures 3(a) and 3(b) show how the capacity and the delay evolve for different frame durations as the distance is increased. Figure 3(a) is obtained with BPSK 1/2, and represents the aggregated UL + DL saturation throughput injecting 1372 bytes UDP packets, with a cyclic prefix of 1/4 and a bandwidth of 10 MHz. The saturation throughput is lower for the shortest frames; however, Figure 3(b) shows how the latency (log scale) in the nonsaturation region in unsaturated WiMAX links is penalized as the frame duration is increased. While a frame duration of 20 ms drives to the highest capacity, the drawback is a delay as high as 42 ms for best-effort traffic.

On the contrary, the shortest frame drives to a very short delay, around 7 ms, but the capacity drops more than 30%. This trade-off should be solved looking first at how much delay can be spent in the WiMAX link, and then choosing the longest frame duration that still keeps the average delay under that limit. In this paper, a 4 ms frame duration is chosen for comparisons. Finally, it is worth stressing that since WiMAX is a TDMA technology, the increase in delay after the saturation point is practically only due to queuing delay originated by the PHY bottleneck.

6.5. Results Obtained for NV2 (A WiFi-Based TDMA Solution). As explained in the previous section, nobody except the manufacturers (i.e., Mikrotik) can propose an analytical model for NV2. However, based on the little existing knowledge about its nature and based also on the experience of many users [36, 37], it is known that the capacity of a long NV2 link drops very slowly and linearly with the distance, just as WiMAX. In absence of theoretical models and simulators, only experimental measurements permit to obtain the performance of NV2 for different MCS. The performance has been measured for 0 km of distance in laboratory (5 m) and for a 30 km link on the field (actual distance 29.8 km). The measurements are done with similar adjustments as in the case of WiLD and a frame duration of 2 ms and due to the restrictions of the link budget, only up to 16 QAM 3/4 could be tested (i.e., MCS4 for SISO and MCS12 for MIMO).

Table 7 shows the saturation throughput for the different MCSs for 0 and 30 km for NV2. Also values for WiLD are shown as reference. In this case, a frame aggregation of 8192 bytes is used, which highly boosters the performance in comparison with the models, specially at the higher MCSs. As can be seen, WiLD behaves at short distances better than NV2 for the different MCSs; however, at 30 km, NV2 renders much higher throughput due to its TDMA MAC layer, as WiMAX does. This is due to that both NV2 and WiMAX can adjust the timers for high-propagation times so that the effects of the distance in the throughput are minimized, while for NV2, there is a performance drop of around 10% for 30 km, in WiLD, this drop in performance is more than 50%. This shows that for long distances, the efficiency is higher for TDMA MAC layers than CSMA MAC layers.

Finally, Figure 4 shows NV2 latency in function of the offered load at 30 km. It can be seen that the range of offered load with low delay is around 60%, which is equivalent to the values in WiLD for frame aggregation $N = 6$, as shown in Figure 2(b). Note that as with WiLD and WiMAX, a traffic load of 100% is equivalent to the maximum nominal rate available in the link.

6.6. Comparison between Different Technologies. Once the three technologies have been characterized in performance for different distances, we compare them subject to the conditions that permit to use them as backhaul for 3G rural networks.

For this reason, Figure 5 compares 802.11n (WiLD), WiMAX, and NV2 in terms of the maximum supported throughput with a delay lower than 5 ms (i.e., unsaturated conditions). Since transport networks are likely multihop, the cumulative nature of the delay enforces us to limit the one-hop delay strongly. This means that 2.5 ms of frame duration is chosen for WiMAX and 2 ms for NV2.

For WiLD, the frame aggregation is set to $N = 6$ since it does not affect the latency in the nonsaturated region. Results are obtained, as before, for bidirectional UDP traffic with 1372 byte payload size. For WiLD and NV2, we use GI = 800 ns and a cyclic prefix of 1/4 for WiMAX. The channels are 20 MHz width for WiLD and for NV2 and

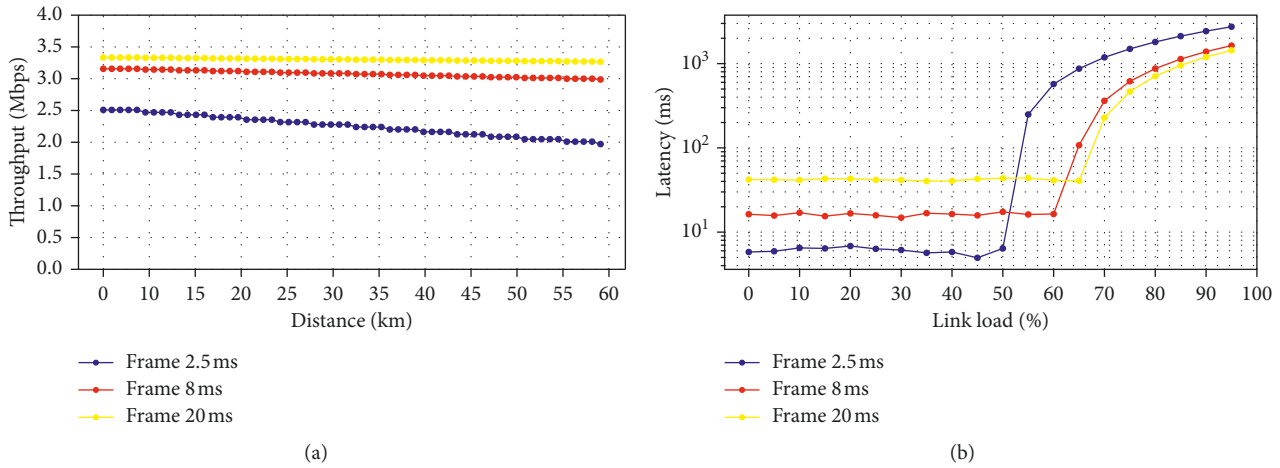

Figure 3: Simulation results for WiMAX. (a) Average saturation throughput values for different frame duration in WiMAX regarding the distance. (b) Average delay values in WiMAX for different frame duration regarding the load at a distance of 30 km.

Table 7: Average saturation throughput values in Mbps obtained in real experiments for NV2 and WiLD for 0 and 30 km.

	0 km	30 km		0 km	30 km
NV2 MCS0	4.35	4.1	WiLD MCS0	6.1	5.8
NV2 MCS1	9.09	8.4	WiLD MCS1	11.2	5.9
NV2 MCS2	13.82	12.8	WiLD MCS2	16.7	6.8
NV2 MCS3	18.57	18.0	WiLD MCS3	22.7	10
NV2 MCS4	27.9	26.6	WiLD MCS4	34.3	15
NV2 MCS5	37.12	—	WiLD MCS5	45	—
NV2 MCS6	41.75	—	WiLD MCS6	50.8	—
NV2 MCS7	45.97	—	WiLD MCS7	55.7	—
NV2 MCS8	10.4	8.8	WiLD MCS8	12.2	6.3
NV2 MCS9	19.2	17.8	WiLD MCS9	24.1	9.6
NV2 MCS10	27.8	26.4	WiLD MCS10	36.2	15.8
NV2 MCS11	37.0	35.3	WiLD MCS11	48.1	19.6
NV2 MCS12	63.5	52.6	WiLD MCS12	71.6	30.8
NV2 MCS13	77.2	—	WiLD MCS13	90.2	—
NV2 MCS14	81.1	—	WiLD MCS14	96.4	—
NV2 MCS15	85.2	—	WiLD MCS15	102.3	—

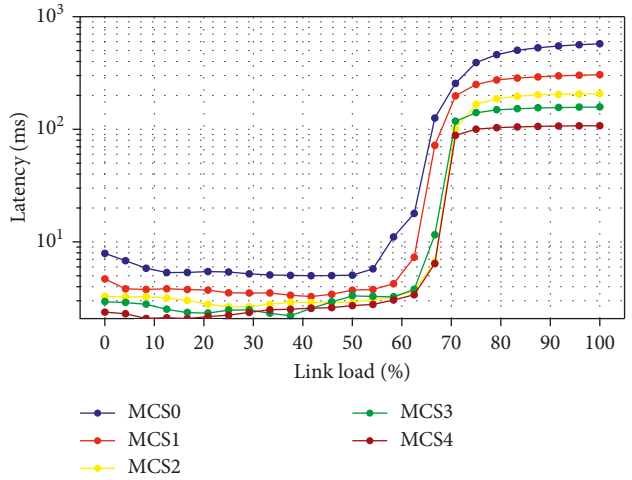

Figure 4: Average delay values obtained for NV2 in experimental tests at 30 km for different offered load.

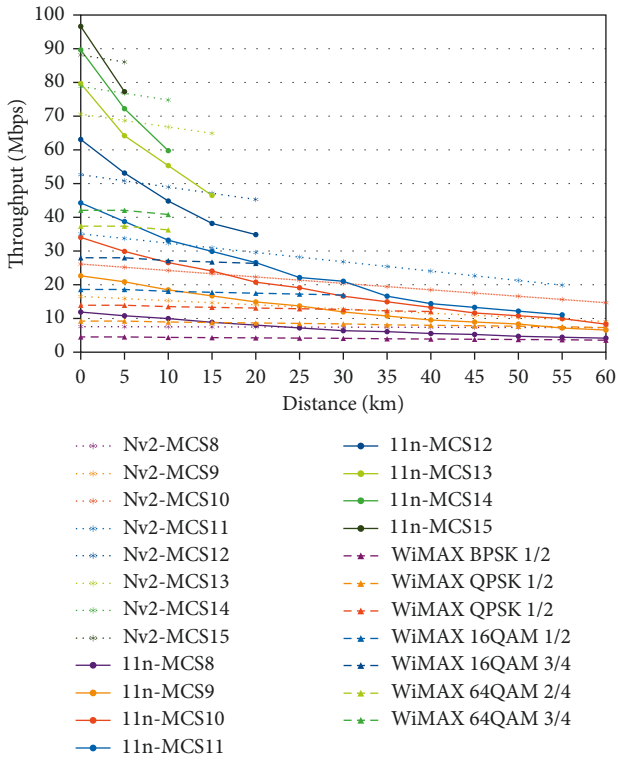

Figure 5: 5 ms delay-bounded throughput comparison between the different technologies obtained from the NS-3 simulator (WiLD and WiMAX) and from the experimental results (NV2).

10 MHz for WiMAX. Since a linear behaviour is expected in the performance of NV2 (as occurs with WiMAX) due to its TDMA-based protocol, we have interpolated NV2 values between 0 and 30 km and between 30 km and 60 km, so that all NV2 values are estimated values but the values at 0 and 30 km.

The best performance at short distances is obtained with WiLD, up to 2-3 km. It is important to notice that, beyond that distance, NV2 is always better than WiLD as already

shown in Table 7. However, the performance of WiMAX is always below WiLD and NV2. This is basically due to the fact that the maximum bandwidth allowed in the IEEE 802.16 standard for WirelessHUMAN is 10 MHz, so that the real capacity is far below the capacity obtained with IEEE 802.11n PHY using 20 MHz channels. Although for all distances and with short frame sizes, WiMAX exhibits the maximum spectrum efficiency, it is not an interesting alternative for backhaul networks since its performance can be easily surpassed by the 20 MHz channels of WiLD and NV2. Only very particular scenarios where high capacity is not required but a strong QoS policy is essential, which could benefit of building WiMAX links. Otherwise, usual QoS requirements in a backhaul networks can fairly be accomplished using WiLD or NV2.

In general, links of 45 Mbps can be obtained at distances up to 20 km with the delay bounded to 5 ms with NV2 when using MIMO and MCS11. This throughput is normally no longer achievable at longer distances since the link budget becomes a significant constraint. For 55 km, NV2 can support up to 20 Mbps. WiLD can only offer 37 Mbps and 10 Mbps at 20 km and 55 km, respectively, with the delay bounded at 5 ms and conditioned to using frame aggregation. Finally, WiMAX can only offer 28 Mbps at 20 km and 8 Mbps at 55 km.

7. Example Use Case

7.1. A Backhaul Solution for 3G Femtocells: A Multihop Network along the Napo River. In order to illustrate that the technologies assessed can be used in a real context, this section presents the network dimensioning for the Napo network use case, one of the scenarios chosen in the TUCAN3G project as proof of concept [3]. Figure 6 shows the topology of this network that is currently deployed with WiLD and NV2 links connecting rural healthcare facilities with the Iquitos' hospital. Hence, the network is a chain of long-distance links in the range of 20–55 km, covering a total end-to-end distance of 450 km approximately. TUCAN3G is deploying a parallel demonstration network reusing the towers from Santa Clotilde to Iquitos, with 3G femtocells in a few villages. The traffic load potentially generated by the villages within the first 5 years of use has been calculated and is shown in Table 8, and compared with the capacity that WiLD, WiMAX or NV2 could be provided in each hop.

The link budget parameters used in the network are the ones shown in Table 6, and the sensitivity figures are shown in Table 5. The Friis propagation model is used for the link budget, and a fading margin of 20 dB has been used in all cases for choosing the modulation and coding scheme with the highest performance in each hop. Also, parabolic dual polarization antennas with 27 dBi gain were used.

Rural backhaul networks have also different peculiarities that require special attention. The lack of power grids in rural areas makes essential the use of alternative power sources such as solar panels and different mechanisms to cope with an unreliable power supply. Also, enclosures have to be minimum 4-4X NEMA type in order to properly protect the equipment from weather conditions and towers

Figure 6: Schema of the rural Napo network, connecting several villages to the city of Iquitos using a set of linearly arranged point-to-point wireless links.

have to be physically secured. These issues were solved by the GTR research group, which have proved experience deploying and operating rural networks [38].

The results in Table 8 show that both WiLD and NV2 provide largely enough capacity for the backhaul requirements of a 3G provider that aims to provide services in these villages. On the contrary, WiMAX would be a valid solution for the four links furthest from the city, but not for the three closest ones. In linear multihop networks, links require more capacity as they are closer to the gateway because they carry the traffic of all the cells that are behind. The Napo network is currently operating with with NV2 since the end of 2016.

Of course, this is only an illustrative example of the feasibility of a multihop transport network based on these technologies, which depends on the specific requirements of this particular scenario. Together with the Balsapuerto Network explained in [6, 7], these two proof-of-concept networks are currently operating with a mix of the referenced technologies supporting 3G femtocells backhaul traffic from different isolated villages.

7.2. Cost and Operation. Regarding the cost of these technologies as backhaul, even though 802.11 and 802.16 systems are inexpensive themselves for operation in nonlicensed bands, both may require expensive infrastructures for long-distance links in flat rural areas due to the high towers required in order to guarantee the LOS. This is particularly important in nonlicensed bands, where the maximum transmission power is strictly limited [9]. This may imply a high CAPEX for some scenarios, while these costs may be substantially lower in mountainous landscapes in which towers may be placed in naturally elevated points. On the other hand, the OPEX is extremely low, which may result in an overall positive balance for WiFi and WiMAX in most real scenarios compared to other more expensive alternatives such as VSAT communications. A more detailed analysis on this can be found in [6].

Regarding the use of nonlicensed bands, their exploitation for a carrier-grade service implies free additional

Table 8: Comparing achievable link capacities with traffic requirements in the Napo network (the acronyms in the links refer to the initials of the locations (see Figure 6)).

Link	Dist. (km)	Mbps req.	WiMAX		WiLD		NV2	
			MCS	Mbps	MCS	Mbps	MCS	Mbps
SC-TC	39.1	6.4	16 QAM 1/2	20.6	MCS12	17.1	MCS12	52.6
TC-NU	25.5	9.2	16 QAM 3/4	15.5	MCS13	31.2	MCS13	70.6
NU-TP	32.2	12.1	16 QAM 3/4	15.4	MCS12	24.9	MCS12	54,0
TP-HU	26.5	14.9	16 QAM 3/4	15.4	MCS13	30.3	MCS13	70.5
HU-M	22.3	17.7	16 QAM 3/4	15.6	MCS13	33.9	MCS13	70.9
M-PP	19.9	24.5	64 QAM 2/3	21.3	MCS13	38.0	MCS13	71.2
PP-HI	11.7	24.5	64 QAM 2/3	21.7	MCS14	41.3	MCS14	74.9

costs, and regulations in many developing countries are evolving towards permitting operators use them in deprived areas. Nonlicense bands are more prone to interferences than licensed bands, even in a rural scenario where RF emissions are scarce. However, since high-directive antennas are used, the nondesired RF power received in the RX antenna can be neglected. In case of scenarios located in countries where licensed bands are mandatory for backhauling carried-grade services, WiMAX is the only low-cost alternative, since it is the only technology of the ones analysed in this work that has a profile that operates in licensed bands. Although the use of licensed bands implies additional significant costs, an operator can still benefit of using a low-cost infrastructure based on WiMAX.

8. Conclusions and Future Works

3G providers usually base their infrastructures on carrier-grade backhaul technologies and macrocells for the access network, driving to solid professional solutions that result to be cost effective in densely populated areas. However, remote rural areas require low-cost technologies that permit the operators to deploy infrastructures in sparsely populated areas and still ensure economical benefits.

Wireless broadband technologies operating in 5 GHz nonlicensed bands are undoubtedly cheaper than traditional carrier-grade backhaul technologies, and the shared spectrum may not be an inconvenient in rural regions. However, there is not common knowledge about the actual performance of WiFi, WiMAX, or WiFi-based TDMA solutions in long-distance links, particularly within backhaul networks, where the traffic is shaped to keep links working under their saturation point in order to bound the delay.

This work has shown that these technologies, and specially 802.11-based TDMA solutions, are a solid solution for rural 3G backhaul links, providing enough capacity and acceptable latency as long as external mechanisms limit the amount of traffic sent through these links [7].

As cited above, standardization bodies such as ETSI BRAN are following this approach. This paper contributes to demonstrate its feasibility, specially focusing in finding the optimum operation point for a link in the curve delay/offered load. This point is usually not the point where maximum throughput is achieved but the point that offers maximum throughput while bounding the delay below 5 ms. The results presented in this paper can be of interest when designing such rural backhaul networks and for implement and operate their traffic control systems.

Data Availability

The source code used to support the findings of this study are included within the article. The simulation and experiment data used to support the findings of this study are available from the corresponding author upon request.

Conflicts of Interest

The authors declare that they have no conflicts of interest.

Acknowledgments

This work has been performed in the framework of the FP7 project TUCAN3G IST-601102 STP, which is funded by the European Community. The authors would like to acknowledge the contributions of the colleagues from TUCAN3G Consortium (http://www.ict-tucan3g.eu). This research has also been partially supported by the Spanish MINECO grant no TEC2013-41604-R.

References

[1] IEEE, "802.11-2012—IEEE standard for information technology exchange between systems local and metropolitan area networks: Wireless LAN Medium Access Control (MAC) and Physical Layer (PHY) specifications," Technical Report IEEE Std 802.11™-2012, IEEE, New York, NY, USA, 802.

[2] IEEE, "802.16-2009—IEEE standard for local and metropolitan area networks part 16: air interface for broadband wireless access systems," Technical Report, IEEE, New York, NY, USA, 2009.

[3] A. Martinez-Fernandez, J. Vidal, J. Simo-Reigadas et al., "The TUCAN3G project: wireless technologies for isolated rural communities in developing countries based on 3G small cell deployments," *IEEE Communications Magazine*, vol. 54, no. 7, pp. 36–43, 2016.

[4] ETSI, "Broadband Radio Access Networks (BRAN); broadband wireless access and backhauling for remote rural communities," Technical Report ETSI TR 103 293, ETSI, Sophia Antipolis, France, 2015.

[5] T. G. Itu, "1010: end-user multimedia QoS categories," Technical Report, ITU, Geneva, Switzerland, 2001.

[6] J. Simo-Reigadas, E. Municio, E. Morgado et al., "Sharing low-cost wireless infrastructures with telecommunications operators to bring 3G services to rural communities," *Computer Networks*, vol. 93, pp. 245–259, 2015.

[7] J. Simo-Reigadas, E. Municio, E. Morgado, E. M. Castro, and A. Martinez, "Sharing low-cost wireless infrastructures with telecommunications operators for backhauling 3G services in deprived rural areas," in *Proceedings of IEEE 16th International Symposium on a World of Wireless, Mobile and Multimedia Networks (WoWMoM)*, pp. 1–8, IEEE, Boston, MA, USA, 2015.

[8] K. Chebrolu, B. Raman, and S. Sen, "Long-distance 802.11 b links: performance measurements and experience," in *Proceedings of the 12th Annual International Conference on Mobile Computing and Networking*, pp. 74–85, ACM, Los Angeles, CA, USA, Sepetember 2006.

[9] J. S. Reigadas, A. Martinez-Fernandez, J. Ramos-Lopez, and J. Seoane-Pascual, "Modeling and optimizing IEEE 802.11 DCF for long-distance links," *IEEE Transactions on Mobile Computing*, vol. 9, no. 6, 2010.

[10] A. Lozano and N. Jindal, "Transmit diversity vs. spatial multiplexing in modern MIMO systems," *IEEE Transactions on Wireless Communications*, vol. 9, no. 1, pp. 186–197, 2010.

[11] F. Bohagen, P. Orten, and G. E. Oien, "Design of optimal high-rank line-of-sight MIMO channels," *IEEE Transactions on Wireless Communications*, vol. 6, no. 4, pp. 1420–1425, 2007.

[12] I. Sarris and A. R. Nix, "Design and performance assessment of high-capacity MIMO architectures in the presence of a line-of-sight component," *IEEE Transactions on Vehicular Technology*, vol. 56, no. 4, pp. 2194–2202, 2007.

[13] C. Oestges, V. Erceg, and A. J. Paulraj, "Propagation modeling of MIMO multipolarized fixed wireless channels," *IEEE Transactions on Vehicular Technology*, vol. 53, no. 3, pp. 644–654, 2004.

[14] L. Jiang, L. Thiele, A. Brylka, S. Jaeckel, and V. Jungnickel, "Polarization characteristics of multiple-input multiple-output channels," in *Proceedings of IEEE 19th International Symposium on Personal, Indoor and Mobile Radio Communications, PIMRC 2008*, IEEE, Cannes, France, September 2008.

[15] J. M. Vella and S. Zammit, "Performance improvement of long distance MIMO links using cross polarized antennas," in *Proceedings of 15th IEEE Mediterranean Electrotechnical Conference (MELECON 2010)*, pp. 1287–1292, Valletta, Malta, April 2010.

[16] B. Raman and K. Chebrolu, "Design and evaluation of a new MAC protocol for long-distance 802.11 mesh networks," in *Proceedings of the 11th Annual International Conference on Mobile Computing and Networking*, pp. 156–169, ACM, Cologne, Germany, August-September 2005.

[17] R. K. Patra, S. Nedevschi, S. Surana, A. Sheth, L. Subramanian, and E. A. Brewer, "WiLDNet: design and implementation of high performance WiFi based long distance networks," *NSDI*, vol. 1, p. 1, 2007.

[18] S. Salmerón-Ntutumu, J. Simó-Reigadas, and R. Patra, "Comparison of MAC protocols for 802.11-based long distance networks," in *Proceedings of Workshop Wireless For Development (WIRELESS4D)*, Karlstad, Sweden, December 2008.

[19] AirMAX TDM SYSTEM, "Product datasheet," December 2018, https://dl.ubnt.com/datasheets/airmax/UBNT_DS_airMAX_TDMA.pdf.

[20] NV2 Manual," December 2018, http://wiki.mikrotik.com/wiki/Manual:Nv2.

[21] G. Bianchi and I. Tinnirello, "Remarks on IEEE 802.11 DCF performance analysis," *IEEE Communications Letters*, vol. 9, no. 8, pp. 765–767, 2005.

[22] I. Tinnirello, G. Bianchi, and Y. Xiao, "Refinements on IEEE 802.11 distributed coordination function modeling approaches," *IEEE Transactions on Vehicular Technology*, vol. 59, no. 3, pp. 1055–1067, 2010.

[23] F. Daneshgaran, M. Laddomada, F. Mesiti, M. Mondin, and M. Zanolo, "Saturation throughput analysis of IEEE 802.11 in the presence of non ideal transmission channel and capture effects," *IEEE Transactions on Communications*, vol. 56, no. 7, pp. 1178–1188, 2008.

[24] F. Daneshgaran, M. Laddomada, F. Mesiti, and M. Mondin, "Unsaturated throughput analysis of IEEE 802.11 in presence of non ideal transmission channel and capture effects," *IEEE Transactions on Wireless Communications*, vol. 7, no. 4, pp. 1276–1286, 2008.

[25] I. Papapanagiotou, G. S. Paschos, S. A. Kotsopoulos, and M. Devetsikiotis, "Extension and comparison of QOS-enabled wi-fi models in the presence of errors," in *Proceedings of Global Telecommunications Conference, GLOBECOM'07*, pp. 2530–2535, IEEE, Washington, DC, USA, December 2007.

[26] D. Senthilkumar and A. Krishnan, "Nonsaturation throughput enhancement of IEEE 802.11 b distributed coordination function for heterogeneous traffic under noisy environment," *International Journal of Automation and Computing*, vol. 7, no. 1, pp. 95–104, 2010.

[27] J. Martin, B. Li, W. Pressly, and J. Westall, "WiMAX performance at 4.9 GHz," in *Proceedings of Aerospace Conference*, IEEE, Big Sky, MT, USA, March 2010.

[28] Ubiquity networks, "Datasheet Nanostation M5 5GHz," December 2018, https://dl.ubnt.com/datasheets/nanostationm/nsm_ds_web.pdf.

[29] Alvarion, "Datasheet 4Motion 802.16e CPE BreezeMAX Si 4000," December 2018, https://www.sourcesecurity.com/datasheets/alvarion-4motion/co-4616-ga/br_4motion_09_2009_rev_g_lr.pdf.

[30] NS3 Network Simulator, December 2018, https://www.nsnam.org/.

[31] A. Botta, A. Dainotti, and A. Pescapè, "A tool for the generation of realistic network workload for emerging networking scenarios," *Computer Networks*, vol. 56, no. 15, pp. 3531–3547, 2012.

[32] R. P. Karrer, I. Matyasovszki, A. Botta, and A. Pescapé, "Magnets-experiences from deploying a joint research-operational next-generation wireless access network testbed," in *Proceedings of 3rd International Conference on Testbeds and Research Infrastructure for the Development of Networks and Communities, TridentCom 2007*, pp. 1–10, IEEE, Lake Buena Vista, FL, USA, 2007.

[33] R. P. Karrer, I. Matyasovszki, A. Botta, and A. Pescapé, "Experimental evaluation and characterization of the magnets wireless backbone," in *Proceedings of the 1st International Workshop on Wireless Network Testbeds, Experimental Evaluation & Characterization*, pp. 26–33, ACM, 2006.

[34] G. Pei and T. R. Henderson, "Validation of OFDM error rate model in ns-3," *Boeing Research and Technology*, Technical Report, 2010.

[35] N. Baldo, M. Requena-Esteso, J. Núñez-Martínez et al., "Validation of the IEEE 802.11 MAC model in the ns3

simulator using the extreme testbed," in *Proceedings of the 3rd International ICST Conference on Simulation Tools and Techniques*, p. 64, ICST, Malaga, Spain, March 2010.

[36] S. Rinaldi, P. Ferrari, A. Flammini, F. Gringoli, M. Loda, and N. Ali, "An application of IEEE 802.11 ac to smart grid automation based on IEC 61850," in *Proceedings of 42nd Annual Conference of the IEEE Industrial Electronics Society, IECON 2016*, p. 4645, IEEE, Florence, Italy, October 2016.

[37] V. Popovskiy, V. Loshakov, O. Philipenko, A. Martinchuk, and A. Drif, "Results of development of tropospheric communications system," in *Proceedings of Second International Scientific-Practical Conference Problems of Infocommunications Science and Technology (PIC S&T)*, pp. 193–195, IEEE, Kharkiv, Ukraine, 2015.

[38] C. Rey-Moreno, I. Bebea-Gonzalez, I. Foche-Perez, R. Quispe-Tacas, L. Liñán Benitez, and J. Simo-Reigadas, "A telemedicine WiFi network optimized for long distances in the amazonian jungle of Peru," in *Proceedings of the 3rd Extreme Conference on Communication: The Amazon Expedition, ExtremeCom '11*, pp. 91–96, ACM, New York, NY, USA, 2011.